*Pol. J. Environ. Stud. Vol. XX, No. X (XXXX), 1-14*
DOI: *10.15244/pjoes/225155* ONLINE PUBLICATION DATE: 2026-08-13

*Original Research*

# Microbial Succession and Related Sulphur Metabolism Pathways in the Treatment of Oily Wastewater from Ships

**Haodong Yi[1, 2], Feifei Chai[1], Xingping Hang[3], Jue Dai[1]*, Xiaoxiao Feng[1], Fangjun Zhao[1], Lu Jiang[3], Shuai Chen[1]****

[1]School of Resources and Environmental Engineering, Shanghai Polytechnic University, Shanghai 201209, China
[2]Zhong An United Coal Chemical Co., Ltd., Huainan 232000, China
[3]Shanghai Chimbusco Marine Bunker Co., Ltd., Shanghai 200080, China

*Received: 26 February 2026*
*Accepted: 27 June 2026*

## Abstract

The microbial succession in activated sludge for the treatment of oily wastewater from ships was investigated by high-throughput sequencing of the 16s rRNA gene, and the microbial metabolic pathways of sulphur were determined. Proteobacteria was the dominant phylum, with a relative abundance of 57.2%-88.0%, and Thiobios and *Thiobacillus* played an important role in the associated sulphur metabolism. Diversity and species differentiation analyses showed that sample A4 after 1 year of domestication had the lowest species diversity. The species with large differences were Thiobios, *SM1A02*, *Thiobacillus*, and *Flavobacterium*. Sulphite oxidation to sulphate occurs through the sulphite oxidase (SO) pathway. Sulphur-oxidising bacteria such as Thiobios and *Thiobacillus* convert sulphite into sulphate through the SO pathway using sulphite-oxidising enzymes. In addition, the sulphite dehydrogenase and reverse heterogeneous sulphate reduction pathways were predicted. These pathways may jointly participate in and regulate the sulphur cycle during the treatment process of oily wastewater from ships. This paper systematically reveals the succession patterns of functional microorganisms in the biological treatment of oily wastewater from ships and the key sulphur metabolic pathways, providing a microbiological basis for optimising the biological treatment process of oily wastewater from ships and enhancing the efficiency of sulphur metabolism.

**Keywords**: oily wastewater, sulphur metabolism, sulphite oxidase, marine environment, microbial succession

*e-mail address: daijue@sspu.edu.cn
**e-mail address: chenshuai@sspu.edu.cn

## Introduction

With the unprecedented development of the global shipping industry, the pollution and ecological damage to the marine environment associated with it are becoming serious. The oily wastewater generated by ships accounts for nearly 30% of a ship's deadweight every year, and the sources mainly include ship bilge water, tanker wash water, ballast water, sludge oil, etc. [1]. In 2018, China's Ministry of Ecology and Environment (MEE) promulgated the Control Standards for Discharge of Water Pollutants from Ships, which require that oily wastewater from ships in inland and coastal waters be collected and discharged into reception facilities and treated onshore. As a result, oily wastewater from docked ships may include desulphurisation scrubber drainage, which contains sulphur from the engine exhaust [2].

Several methods are used for the onshore treatment of oily wastewater from ships, including chemical [3], physical [4], and biological [5] methods. Among them, biological methods are widely used because of their advantages, such as low cost. Chipasa et al. [6] combined the processes of gravity separation, coagulation, flotation, and biochemistry to achieve effective treatment of oily wastewater. Kang et al. [7] developed a fixed membrane bioreactor by combining the processes of hydrolytic acidification and contact oxidation. The chemical oxygen demand (COD) of the effluent was reduced by 74.8%, total suspended substances (TSS) were reduced by 90.9%, and oil was removed by 80.6% at a hydraulic retention time (HRT) of 15 h. Vyrides et al. [8] treated bilge oily wastewater using anaerobic granular sludge and aerobic bacterial agents, respectively, and found that 65% COD removal could be achieved in 13 days.

The International Maritime Organization (IMO) has strict regulations on the sulphur content of marine fuels, but combustion exhaust may enter oily wastewater from ships through scrubbers. The sulphur components in the exhaust are collected in this wastewater and can be transformed by microbial action into hydrogen sulphide or other metabolic products, thereby influencing microbial community succession and the operational stability of biological treatment systems. Meanwhile, the salinity of oily wastewater from ships has a particularly significant influence on sulphur removal performance [9]. Autotrophic denitrifying sulphur-oxidising bacteria, mainly including species such as *Thiobacillus denitrificans*, *Thiomicrospira denitrificans*, *Thiobacillus versutus*, and *Thiosphaera pantotropha*, can use the oxidised forms of nitrogen (nitrate or nitrite) as electron acceptors for energy conservation and bacterial growth, and derive energy from the oxidation of a variety of reduced inorganic sulphur species ($S^{2-}$, $S^0$, $SO_3^{2-}$) [10]. The final products of sulphide oxidation are elemental sulphur or sulphates [11]. In contrast, sulphate-reducing bacteria, which mainly belong to the families Desulfobacteraceae, Desulfobulbaceae and Syntrophobacteraceae, reduce sulphate to sulphide and produce nitrogen gas [12]. Identifying key microbial groups involved in sulphur transformation during the treatment of oily wastewater from ships and determining the dominant microorganisms are crucial for understanding the treatment process. However, there is currently a lack of understanding of the succession of microbial communities in activated sludge used for treating oily wastewater from ships or the metabolic pathways of sulphur. We hypothesise that both sulphite oxidation and sulphate reduction pathways are involved in the treatment processes for oily wastewater from ships.

In this study, we monitored a treatment plant for oily wastewater from ships for 1 year, sampled the sludge 4 times, used 16s rRNA high-throughput sequencing to explore changes in the microbial community, and analysed the data at each taxonomic level to determine the pattern of microbial succession. Inter-sample and inter-generic variability was also analysed using α- and β-diversity analyses. Relationships between chemical variables, genera, and α-diversity indices were explored using redundancy analysis (RDA), and metabolic pathways for the conversion of sulphite to sulphate were predicted using the Kyoto Encyclopedia of Genes and Genomes (KEGG) database. The sulphite oxidase (SO) pathway was identified using barium chromate spectrophotometry and titanium salt spectrophotometry. The anabolic sulphur reduction and cysteine synthesis pathways were predicted using the KEGG database. The results of this study further clarified the process of microbial sulphur metabolism in oily wastewater from ships and broadened our knowledge of the treatment of sulphur-containing wastewater in treatment plants for oily wastewater from ships.

## Materials and Methods

### Sampling Conditions and Basic Indicators of Water Quality

This project was commissioned for an oily wastewater treatment plant for ships in East China. The required treatment capacity was 12.5 $m^3/h$, and the maximum daily sewage treatment capacity was 300 $m^3$. The treatment process was as follows: flocculation and sedimentation → flotation → ozonation → anoxic-oxic (A/O). Samples A1, A2, A3, and A4 were collected from aerobic sludge. To maximise seasonal representativeness, sampling was conducted on 10 August 2023, 13 October 2023, 15 December 2023, and 9 April 2024, corresponding to periods exhibiting typical seasonal characteristics throughout the year. Each sample was obtained by collecting aerobic sludge from two sites and then mixing the samples. This sampling strategy was designed to capture the potential effects of seasonal environmental variation, particularly temperature, on microbial community

dynamics. The influent wastewater consistently contained seawater-related streams, including bilge water and exhaust gas scrubber effluents, resulting in relatively stable but elevated salinity throughout the study period. In contrast, ambient temperature exhibited clear seasonal variation and was considered a key driver of microbial succession. Therefore, the selected sampling times allowed for a systematic assessment of temporal and environmental influences on microbial community structure and sulphur metabolism. The sampling locations were situated in Shanghai, China. The sampling temperatures were 31.3ºC, 28.9ºC, 15.1ºC, and 20.3ºC. The salinity ranged from 5,522 to 5,534 mg/L. The water quality indicators are shown in Table 1.

### Reagents

Potassium dihydrogen phosphate (≥99%), hydrochloric acid (36%), oxalate (≥98%), potassium permanganate (≥99%), ammonium chloride (≥99%), calcium chloride (≥99%), ferrous sulphate (≥99%), titanium dioxide (≥99%), magnesium chloride (≥99%), copper chloride (≥99%), manganese sulphate (≥99%), hydrogen peroxide (30%), ammonium sulphate (≥99%), sodium sulphate (≥99%), potassium chromate (≥99%), barium chloride (≥99%), aluminium chloride (≥99%), and cobalt chloride (≥99%) were obtained from Sinopharm Chemical Reagent Co., Ltd.

### High-Throughput Sequencing Methods for Microbial Communities

DNA from aerobic sludge was extracted using the OMEGA Soil DNA Kit. The highly variable V3-V4 region of the bacterial 16S rRNA gene, approximately 468 bp in length, was used for sequencing (primers: ACTCCTACGGGGAGGCAGCA; GGACTACHVGGGTWTCTAAT). After PCR amplification and purification, the sequencing was performed using the Illumina MiSeq platform. The raw data were then preprocessed using Trimmatic, FLASH and Vsearch software. Sequence similarity was determined by classifying sequences into operational taxonomic units (OTUs). The OTUs were annotated and bioinformatically analysed using QIIME, Greengenes and Ribosomal Database Project (RDP) classifier software.

### Sludge Cultivation Conditions

A model aerobic sludge tank was used to determine the sulphur metabolism pathway. The sludge concentration was 3-3.5 g/L, and the sludge volume index was 80-100 mg/L. The influent matrix consisted of the following substances in addition to the sludge (mg/L) $NH_4Cl$: 200; $KHPO_4$: 50; $CaCl_2$: 50; $MgCl_2$: 40; $FeSO_4$: 10; $CuCl_2$: 0.03; $AlCl_3$: 0.05; $CoCl_2$: 0.05; $NiCl_2$: 0.05. The operation times were as follows (min): influent, 5; anaerobic retention, 20; aeration, 310; sedimentation, 5; drainage, 20.

### Analytical Methods

The sulphate concentration in water was measured using the chromium barium spectrophotometry method according to the national standard (Standard No. HJ/T 342-2007). With an absorption peak at 420 nm, the absorbance can be measured to determine the sulphate concentration. The hydrogen peroxide concentration in water was determined using the titanium salt colourimetric method according to the national standard (Standard No. GB 5009 226-2016). There is an absorption peak at 430 nm, and its absorbance value can be measured to determine the hydrogen peroxide concentration. Both methods used the Shanghai Yuanxi UV-5800PC spectrophotometer for detection. Sulphite concentration was measured using a Thermo Fisher Scientific AQ-1200 ion chromatograph (IC).

## Results and Discussion

### Differences in Microbial Abundance at Each Level

The species information for the four samples was summarised using Krona species composition analysis and the results are shown in Fig. 1. It was found that Proteobacteria, especially α-Proteobacteria, β-Proteobacteria and δ-Proteobacteria, constituted the dominant flora in the community. Tian et al. [13] found a high abundance of the phylum Proteobacteria in the microbial community of oily wastewater from long-term drip irrigation. Wang et al. [14] studied the microbial community in petroleum-contaminated groundwater and found that Proteobacteria and Firmicutes together

Table 1. Water quality indicators for biochemical tanks.

| Sample ID | pH | COD (mg/L) | $BOD_5$ (mg/L) | TN (mg/L) | TP (mg/L) | Sulphate content (mg/L) |
|---|---|---|---|---|---|---|
| A1 | 7.4 | 840 | 320 | 115 | 45 | 520 |
| A2 | 7.5 | 830 | 230 | 110 | 40 | 510 |
| A3 | 7.4 | 920 | 350 | 140 | 50 | 610 |
| A4 | 7.9 | 1080 | 325 | 80 | 25 | 640 |

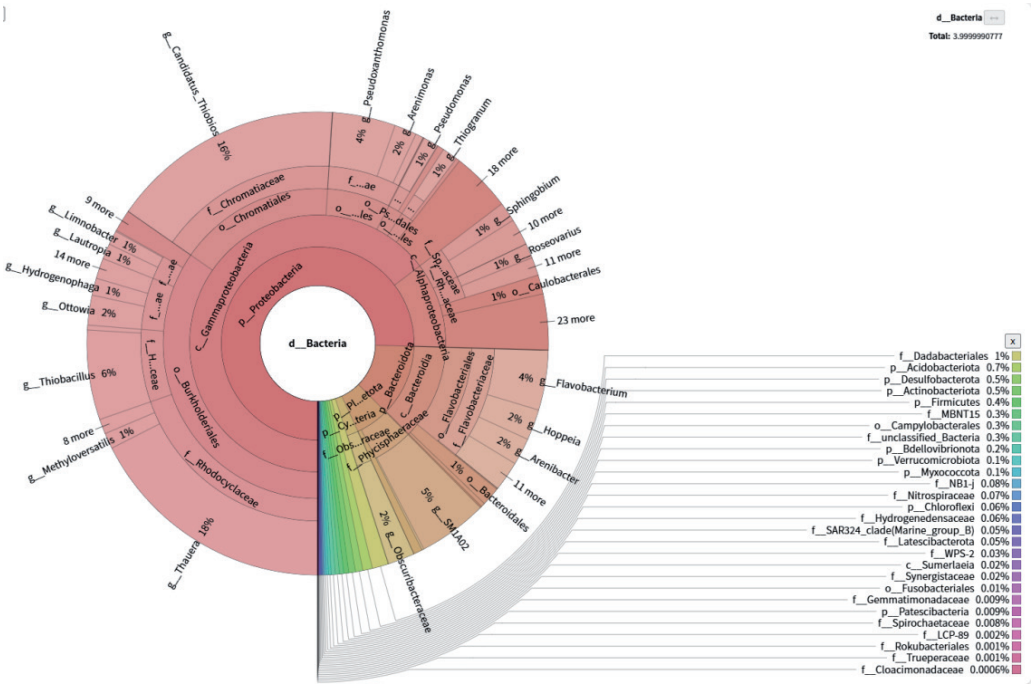


Fig. 1. Krona species composition map.

could reach 96.45%, and Proteobacteria was the most abundant phylum in all samples. Among them, the orders Chromatiales, Burkholderiales, and Xanthomonadales were the major taxa. In addition, Thiobios, *Thiobacillus*, *Thauera*, and *Flavobacterium* accounted for 16%, 6%, 18%, and 4% of the total, respectively, and these species are also frequently found in oily wastewater systems [15].

## Differences in Microbial Abundance at the Phylum Level

As shown in Fig. 2a), Proteobacteria and Planctomycetota were the dominant microbial phyla with relative abundances of 70.9% and 18.7%, respectively, in sample A1. In addition, Cyanobacteria (4.9%) and Bacteroidota (1.5%) were also present. In sample A2, Proteobacteria and Planctomycetota dominated with contents of 88.0% and 2.9%, respectively, and Bacteroidota (1.5%) and Cyanobacteria (2.5%) were also included. In sample A3, Proteobacteria and Bacteroidota dominated with 57.2% and 34.3%, respectively. There were also Dadabacteria (2.7%) and Actinobacteriota (1.6%). In sample A4, Proteobacteria and Bacteroidota dominated with 85.7% and 10.9%, respectively, and Desulfobacterota accounted for 1.6% of the total.

Bacteroidota dominated both A3 and A4. In particular, the relative abundance was as high as 34.3% in A3, which is consistent with the study by Su et al. [16]. This is due to lower temperatures during the sampling period in late December. The relative abundance of Proteobacteria decreased with decreasing temperature, from 88% in sample A2 to 57.2% in sample A3, which is consistent with the findings of Sposob et al. [17]. This is largely consistent with the fact that the city of Shanghai undergoes an autumn to winter transition from October to December each year, resulting in a sudden drop in temperature.

Although the microbial community underwent some changes over time, Proteobacteria were still the dominant organisms. The δ-amoebae in the Proteobacteria included the basically aerobic substrate-forming slime molds as well as several strictly anaerobic species, such as *Desulfovibrio*, *Desulfobacter*, *Desulfococcus*, *Desulfonema* and *Desulphuromonas* among the sulphate-reducing bacteria [18]. *Desulfovibrio* and other desulphurisation bacteria among the sulphate-reducing bacteria can reduce sulphate to hydrogen sulphide using lactic acid, pyruvic acid, ethanol or certain fatty acids as carbon and energy sources [19].

## Differences in Microbial Abundance at the Genus Level

Fig. 2b) depicts the distribution of microbial abundance at the genus level. It can be seen that Thiobios and *SM1A02* were the dominant genera at the time of sampling in the summer in A1, with contents of 30.3% and 17.2%, respectively. In addition, *Thauera* also accounted for a considerable proportion, at 10.8%. Thiobios is a sulphur-oxidising bacterium, which belongs to the sulphur-autotrophic group of bacteria that usually forms a symbiotic relationship with certain marine organisms, and this bacterium plays an important role in marine ecosystems, especially in the sulphur and nitrogen cycles [20]. *Thauera* is a member of the β-subclass of the Proteobacteria, and is widely

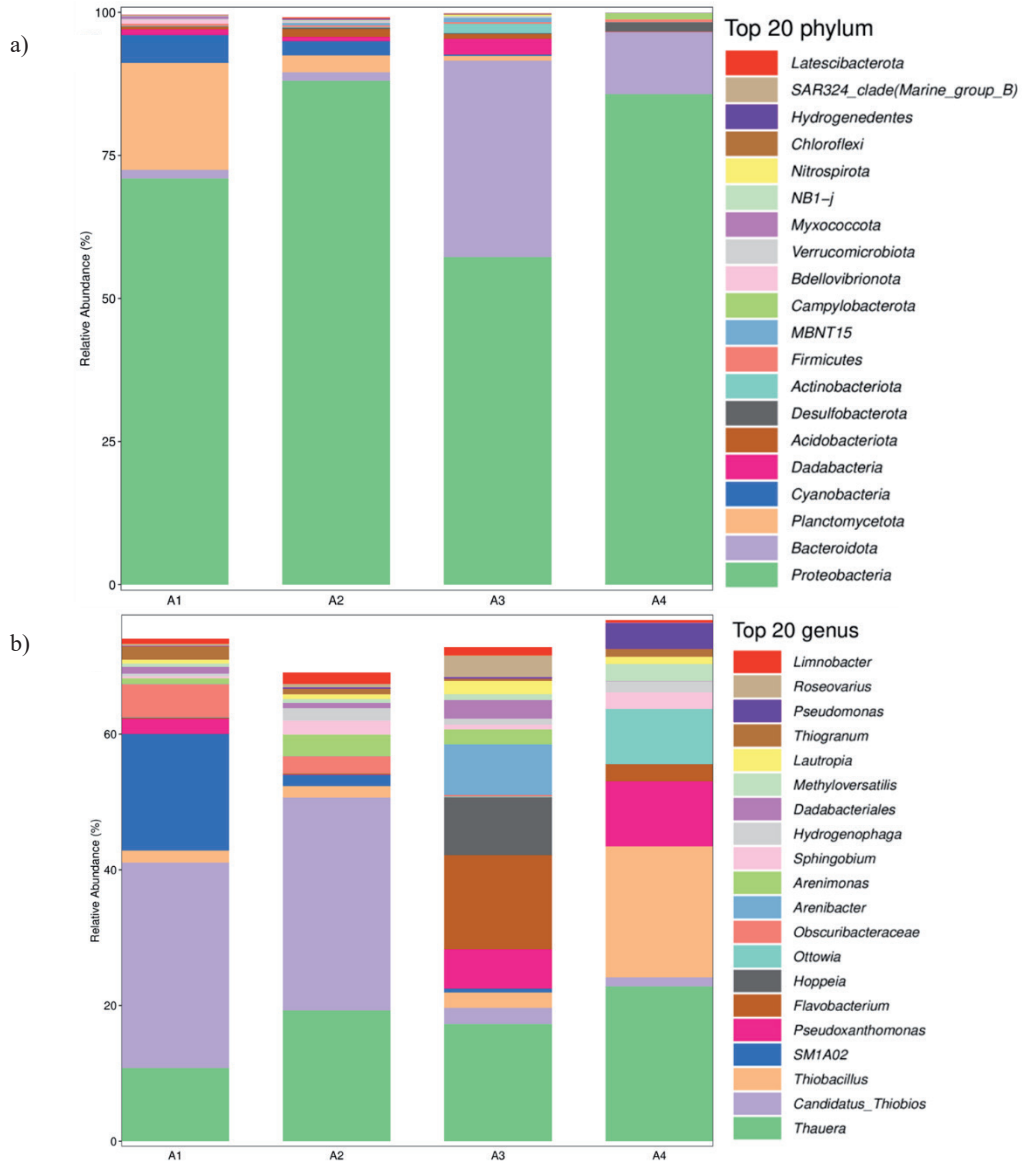


Fig. 2. a) Species abundance map at the phylum level and b) species abundance map at the genus level.

present in various types of biological wastewater treatment processes and has the ability to degrade a wide range of aromatic pollutants [21]. In sample A2, Thiobios and *Thauera* were the dominant genera during autumn sampling, with relative abundances of 31.4% and 19.3%, respectively. *Arenimonas* was also notable, with a percentage of 3.2%. In sample A3, Thiobios was no longer the dominant genus in the winter, and the dominant genera became *Thauera* and *Flavobacterium*, with a percentage of 17.3% and 13.9%, respectively. In addition, *Hoppeia* and *Arenibacter* accounted for 8.5% and 7.5%, respectively. Most species of *Flavobacterium* are harmless and utilise organic substrates such as proteins and polysaccharides, but some members may play an important role in the cycling of organic matter in their environment [22]. *Flavobacterium* is found in a wide variety of environments, including freshwater, marine, and soil environments, and is known for its ability to degrade complex organic compounds and is often identified by its characteristic yellow-orange colour [23]. During the spring sampling in A4, *Flavobacterium* was no longer the dominant genus but rather *Thiobacillus* and *Thauera*, with contents of 19.3% and 22.8%, respectively. *Pseudoxanthomonas* and *Ottowia* were also notable, with contents of 9.6% and 8.1%, respectively. *Thiobacillus* is a sulphur-oxidising bacterium that mainly plays an oxidising role, which can oxidise sulphides to monomeric sulphur or sulphate, or oxidise thiosulphate to sulphate [24].

Oily wastewater from ships had a high sulphate concentration of 520-640 mg/L, and based on the high abundance of *Thiobacillus* and Thiobios at the genus level in all four samples, it is assumed that the sludge contained high sulphide levels over an extended period and that the microorganisms underwent corresponding community succession in wastewater with a high sulphur content.

## Microbial Diversity Analysis

As shown in Table 2, A2 had the highest species richness and A4 had the lowest richness (Chao1 index). The Shannon and Simpson indices showed that species diversity was highest in A3 and lowest in A4 among the four samples. Pielou's evenness index showed that the species distribution was the most even in A3. Good's coverage index indicated that the four sampling times were sufficient to reflect most of the bacterial community information in the samples, and also indicated that the sequencing depth requirement was satisfied [25]. The α-diversity index associated with A4 was generally low, whereas the differences among the other three samples were not very large. This was generally consistent with the water quality indices mentioned above. In A4, the total phosphorus (TP), total nitrogen (TN), COD, $BOD_5$, and pH indicators changed; the $BOD_5$/COD ratio was 0.3, and biodegradability was slightly poorer than in the other samples. This may have caused the microbial community in the sludge to become less diverse, resulting in lower α-diversity. Ye et al. [26] also found that the α-diversity index showed a positive correlation with water quality indicators.

## Analysis of Species Variability

As shown in Fig. 3a) and b), Principal Component Analysis (PCA) was used to extract two principal components from microorganisms in oily wastewater from ships over 1 year. The variance contribution rates of the first and second principal components were 69.1% and 21.8%, respectively, and the cumulative variance contribution of the two principal components was 90.9%, which explained most of the information represented by the original variables. The genera showing large differences in Fig. 3a) were Thiobios, *SM1A02*, *Thiobacillus*, and *Flavobacterium*. Among the four samples shown in Fig. 3b), A1 and A2 were closer, indicating that the microbial communities in these two seasons were more similar. Moreover, A1 and A2 were farther from the other measurement points, A3 and A4, indicating that they differed more from the other samples.

## Correlation of Microbiological and Chemical Variables

The relationships between chemical variables, genera and α-diversity indices are shown in Fig. 4a) and b). The RDA model showed that the contribution of the eigenvalues of the RDA1 and RDA2 axes amounted to 43.52% and 40.61%, respectively, while the total contribution of the first two axes was 84.13%. It can be seen that there were positive correlations between TP, TN, COD, BOD5, pH, and sulphate content, as well as between Simpson's index and Shannon's index. As shown in Fig. 4a), A4 was positively correlated with TP, TN, COD, BOD5, pH, and sulphate content, while A3 was positively correlated with Simpson's index and Shannon's index. It is noteworthy that Simpson's index and the Chao1 index had the greatest influence on microbial community structure. The larger the circle representing a species in the diagram, the higher its microbial abundance. This indicates that Thiobios, *Thauera* and *Thiobacillus* exhibit relatively high abundance, while *Flavobacterium*, *SM1A02*, and *Hoppeia* also demonstrate significant abundance. A sharp angle between a species and an environmental factor indicates a certain degree of correlation between them. As shown in Fig. 4b), the angle formed between the genera *Thiobacillus* and Thiobios and sulphate content is acute, indicating a significant positive correlation. This suggests that sulphate levels in sludge are intrinsically linked to these sulphate-reducing bacteria. Furthermore, *Thauera*, a typical wastewater treatment bacterium, also exhibits a marked positive correlation with these water quality indicators. Marie et al. [27] found a close relationship between physicochemical parameters of water quality, bacterial indicators, and months, indicating that microbial survival depends on environmental and climatic conditions. Qi et al. [28] found that temperature, dissolved oxygen, electrical conductivity, COD, TP, TN, ammonia nitrogen ($NH_3$-N) and microbial communities were closely related to each other.

## Metabolic Pathway Statistics

Fig. 5 is a histogram showing the distribution of KEGG secondary functional pathway abundance based on PICRUSt2 prediction results. In terms of metabolism, it can be seen that the oily wastewater from ships has

Table 2. Results of the α-diversity analysis.

| Sample | Chao1 | Simpson | Shannon | Pielou_e | Faith_pd | Goods_coverage |
|---|---|---|---|---|---|---|
| A1 | 1666.69 | 0.905697 | 6.05235 | 0.567925 | 89.0485 | 0.995404 |
| A2 | 1742.74 | 0.920104 | 6.92778 | 0.647619 | 75.2514 | 0.994669 |
| A3 | 1493.29 | 0.964637 | 6.91379 | 0.655871 | 75.8611 | 0.998918 |
| A4 | 481.128 | 0.933669 | 5.44719 | 0.616766 | 34.6445 | 0.998839 |

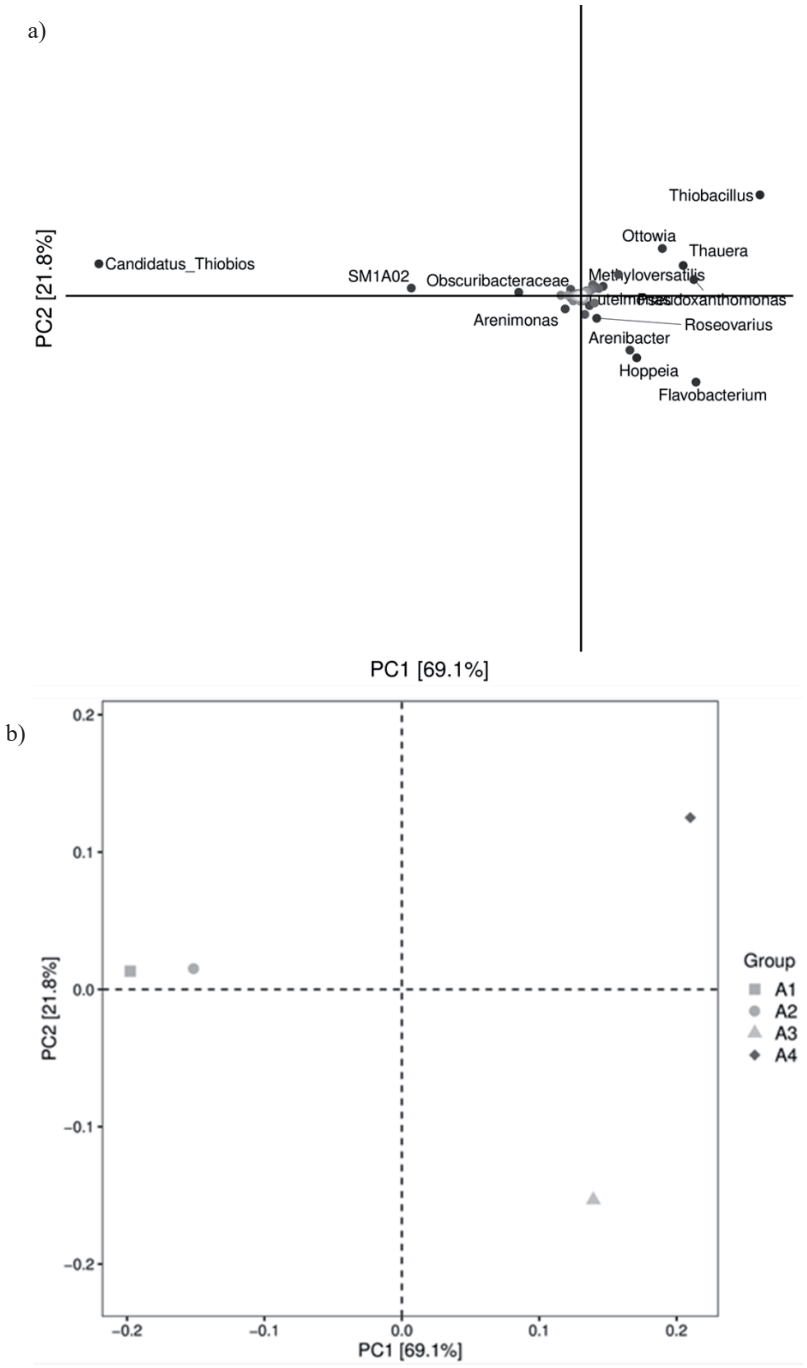


Fig. 3. a) Plot of PCA differences between genera and b) between samples.

a relatively high abundance of amino acid metabolism, carbohydrate metabolism, copolymer metabolism, and vitamin metabolism. Among the biodegradation and metabolism of exotic organisms, the gene abundance in A4 is significantly higher than that in A1. Terpene and polyketide metabolism, lipid metabolism, carbohydrate metabolism, and amino acid metabolism were more abundant in A3. Sulphur metabolism was an energy metabolism pathway, which also showed high abundance [29].

## Prediction of Relevant Sulphur Metabolic Pathways

It was evident from the previous sections that the scrubber effluent from ships contained high levels of sulphides and a high abundance of Thiobios and *Thiobacillus*. This represents a high level of sulphides in the oily wastewater from ships. As was shown in Fig. 6a), the wastewater contained significant amounts of sulphite and sulphate ions. In order to explore how sulphite is converted to sulphate by sulphur-oxidising bacteria, the KEGG database was used to determine the abundance of functional genes involved in sulphite oxidation.

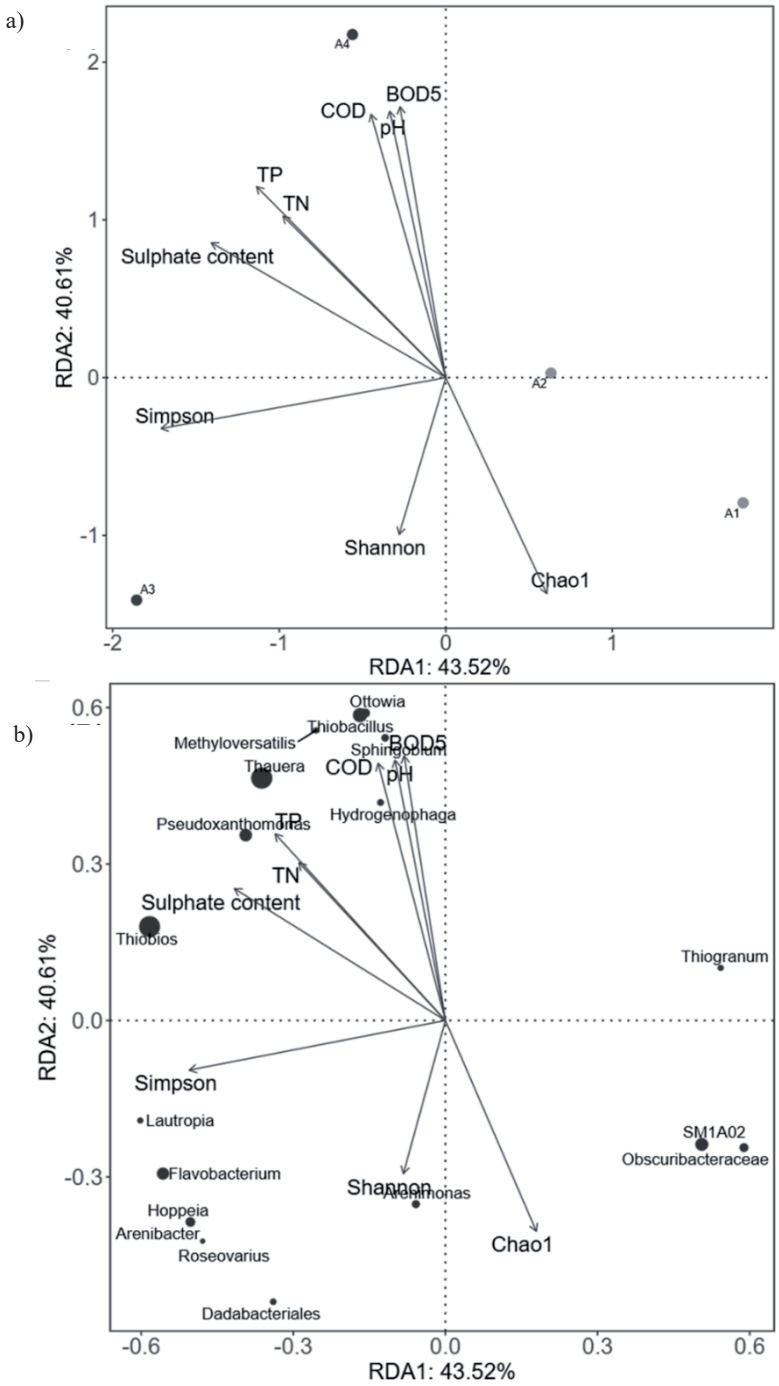


Fig. 4. a) Relationship between the sample and individual indicators and b) between attributes and individual indicators.

As shown in Table 3, the genes participating in the SO pathway included sorA, SUOX, sat, aprA, and aprB [30]. The results of gene abundance analysis showed that the abundances of the aprA and aprB genes in the four samples were basically the same. The gene abundance of the SUOX gene in the four samples was generally higher, and the gene abundance of A4 was as high as 734.5. This is likely to account for a larger proportion of the conversion of sulphite to sulphate by the sulphite oxidase encoded by the SUOX gene.

Sulphite oxidase is one of the five known molybdenum-containing enzymes in eukaryotes that catalyses the oxidation of sulphite to sulphate. Almost all sulphite oxidases (SOEs) are enzymes with 'molybdenum' as a cofactor, and are often referred to as "Mo-Co" proteins [31]. There are two main forms of SOE: (1) the SO pathway which uses $O^2$ as an electron acceptor to catalyse the reaction of sulphite binding to water to produce sulphate and hydrogen peroxide, and (2) the SDH pathway, which replaces $O^2$ with another electron acceptor, cytochrome c, to produce sulphate and reduced cytochrome c [32]. Bacteria can also oxidise sulphite to sulphate via the reverse heterogeneous sulphate reduction pathway. A total of three pathways

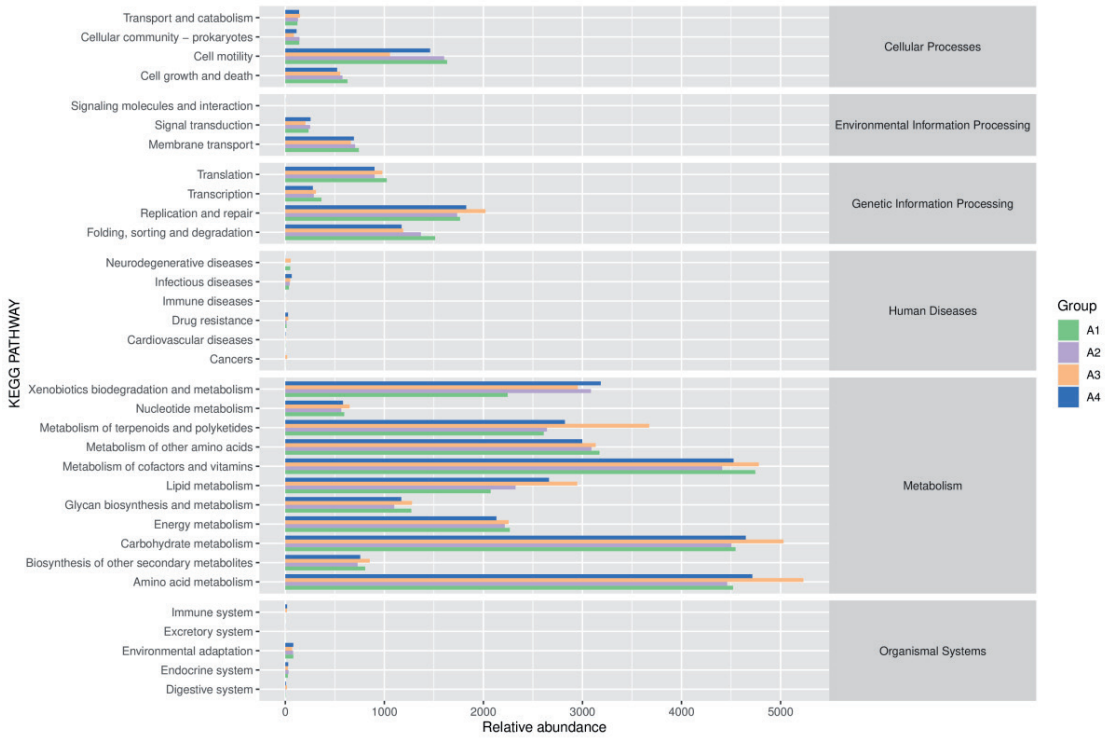


Fig. 5. Functional potential prediction map.

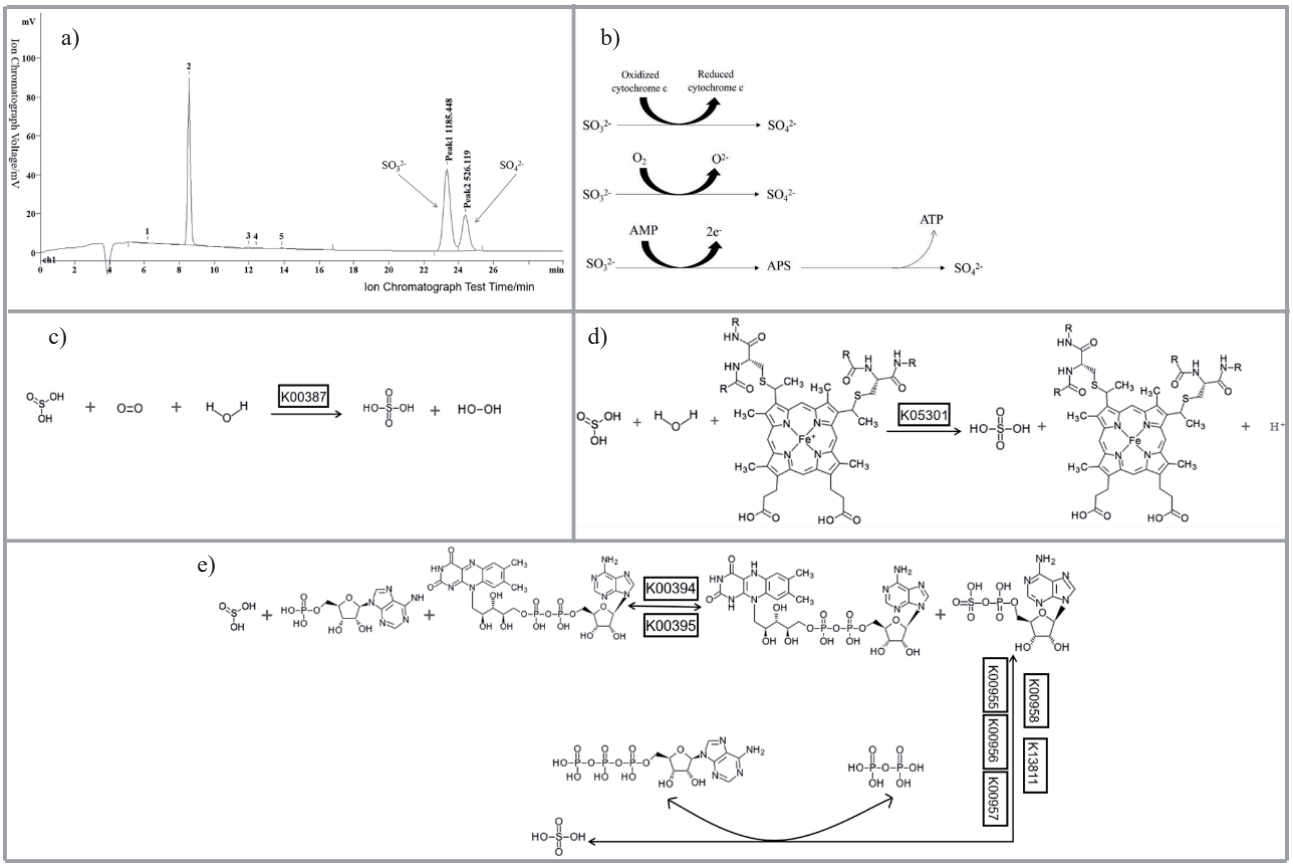


Fig. 6. a) Ion chromatograph diagram, b) diagram of the three pathways of sulphur metabolism, c) diagram of the SO pathway, d) diagram of the SDH pathway and e) diagram of the pathway of reverse heterogeneous sulphate reduction.

Table 3. Sulphite oxidation gene and enzyme-related abundances.

| Gene name | KEGG ID | Enzymes encoded | A1 | A2 | A3 | A4 |
|---|---|---|---|---|---|---|
| sorA | K05301 | Sulphite dehydrogenase (cytochrome) subunit a | 45.2642 | 105.124 | 112.167 | 127.595 |
| SUOX | K00387 | Sulphite oxidase | 556.2 | 643.3 | 672.1 | 734.5 |
| sat | K00958 | Sulphate adenylyltransferase | 239.9 | 287.531 | 92.0289 | 32.8754 |
| aprA | K00394 | Adenylylsulphate reductase, subunit a | 189.82 | 158.601 | 16.0809 | 10.4324 |
| aprB | K00395 | Adenylylsulphate reductase, subunit b | 189.83 | 158.599 | 16.0812 | 10.4326 |

for the conversion of sulphite to sulphate are shown in Fig. 6b).

The first pathway is shown in Fig. 6c). Sulphite reacts with oxygen and $H_2O$ to form sulphate and hydrogen peroxide in the presence of the enzyme K00387 [33]. The second pathway is shown in Fig. 6d). Sulphite binds $H_2O$ and cytochromes to produce sulphate, reduced cytochrome c and $H^+$ by the action of K05301 [34]. The third pathway is the reverse heterogeneous sulphate reduction pathway. As shown in Fig. 6e), sulphite reacts with adenosine monophosphate and flavin adenine dinucleotide to form adenosine sulphate and FADH2 in the presence of enzymes K00394 and K00395. Subsequently, adenosine sulphate reacts with diphosphate in the presence of enzymes K00955, K00956, K00957, K00958, K13811, and ATP and sulphate are generated. Zhou et al. [35] proposed the heterogeneous sulphate pathway as: Sulphate → APS → Sulphite → Sulphide. This is identical to the reverse heterogeneous sulphate reduction process, in which sulphite is converted to sulphate.

## Inference of SO metabolic pathways

In order to better demonstrate that sulphite is converted to sulphate in microorganisms through these three pathways, barium chromate spectrophotometry was used to measure the change in sulphate content in the sludge, and the titanium salt colourimetric method was used to test hydrogen peroxide concentration. After several days of continuous dosing of 200 mg/L sulphite per day into the biochemical tank, the changes in hydrogen peroxide concentration are shown in Fig. 7. The sulphate content gradually increased, which is consistent with the hypothesis that sulphite is converted to sulphate. With the gradual addition of sulphite, the concentration of hydrogen peroxide in the biochemical tank also increased gradually. The sulphite concentration increased from 548 mg/L to 1540 mg/L, and the hydrogen peroxide content increased from 10 μg/mL to 55 μg/mL.

According to previous studies, hydrogen peroxide has an antimicrobial effect, and its effect on bacteria is specifically manifested in its ability to act as an

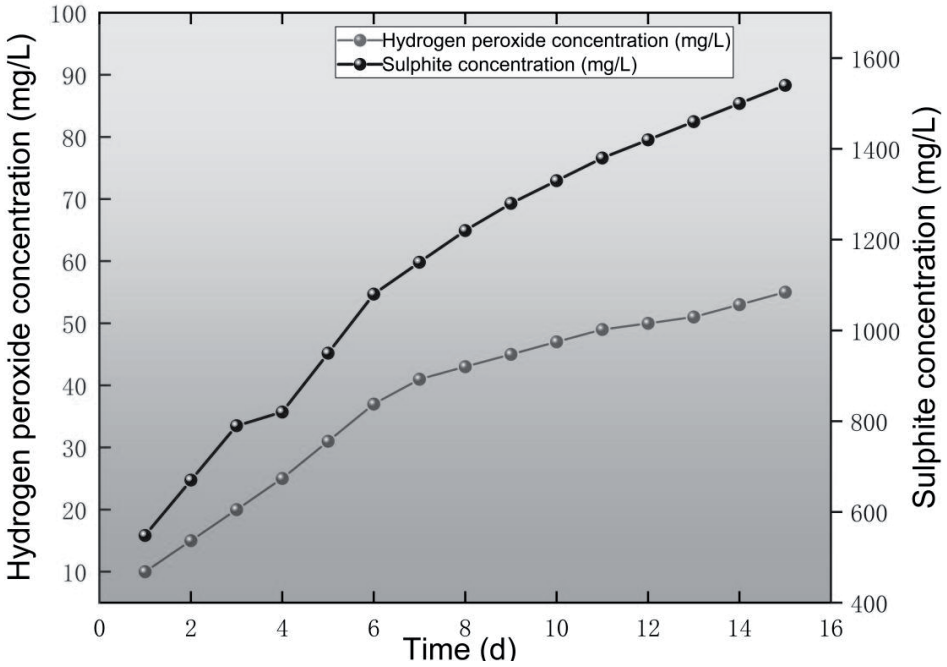


Fig. 7. Changes in hydrogen peroxide and sulphite concentrations.

intermediate in oxygen reduction to produce more reactive and cytotoxic oxygen species, such as hydroxyl radicals, which are strong oxidising agents that can trigger oxidation and cause damage to nucleic acids, proteins and lipids [36]. For many species of bacteria, catalase is the most important protective system against high concentrations of hydrogen peroxide [37]. The detoxification capacity of catalase may protect organisms from oxidative bursts of neutrophils and other immune-responsive inflammatory cells [38]. It is hypothesised that it is the protective mechanism of catalase that thereby allows microorganisms in sludge to survive large variations in hydrogen peroxide concentration over short periods of time. Elevated concentrations of hydrogen peroxide and sulphite in the sludge suggest that sulphur-oxidising bacteria like Thiobios and *Thiobacillus* convert sulphite to sulphate in the SO metabolic pathway.

## Prediction of Sulphur Reduction Metabolic Pathway

The Desulfovibrio phylum of A4, mentioned earlier, also occupied 1.6% of the total, and contains a number of Desulfovibrio bacteria that can carry out assimilatory sulphate reduction metabolism. Although they occupied a small percentage, it is presumed that a small percentage of anaerobic reactions were still carried out in the aeration dead space of the sludge. When this hypothesis was evaluated using the KEGG PATHWAY database, after the relevant enzyme genes were compared, as shown in Table 4, it was found that M00176, the pathway for the conversion of sulphate into hydrogen sulphide, contains all the related enzyme genes, and completes the metabolism of sulphur reduction. The KEGG PATHWAY database and the test results were combined to analyse the sulphur reduction pathway in microorganisms, and the degradation pathway is shown in Fig. 8a).

Sulphate combines with ATP to produce diphosphate and adenylate sulphate in the presence of the enzymes K13811, K00955, K00956, K00957 (sulphate adenylyltransferase subunit 2), and K00958. A portion of this adenylate sulphate binds to ATP to generate ADP and 3-phosphoadenosyl sulphate in the presence of enzymes K00860, K00955, and K13811. Subsequently, 3-phosphoadenosyl sulphate binds to thioredoxin in a reaction that generates thioredoxin disulphide, sulphite, and adenosine 3,5-diphosphate in the presence of the enzyme K00390. In addition, there is a portion of adenosine sulphate that binds glutathione to generate AMP, sulphite, and glutathione disulphide in a redox reaction under the action of the enzyme K05907. The sulphite generated by the two pathways will combine with hydrogen ions to generate hydrogen sulphide and NADP under the action of K00380 and K00381, respectively. Furthermore, sulphite also combines with

Table 4. Abundance of enzymes related to assimilatory sulphate reduction.

| Enzyme number | Enzyme name | Abundances | | | |
|---|---|---|---|---|---|
| | | A1 | A2 | A3 | A4 |
| K13811 | PAPSS; 3'-phosphoadenosine 5'-phosphosulphate synthase | 2.56707 | 8.17492 | 7.44025 | 0.4582 |
| K00955 | cysNC; bifunctional enzyme CysN/CysC | 212.184 | 178.414 | 169.512 | 244.63 |
| K00956 | cysN; sulphate adenylyltransferase subunit 1 | 100.564 | 178.968 | 369.022 | 349.932 |
| K00957 | cysD; sulphate adenylyltransferase subunit 2 | 320.046 | 365.804 | 538.26 | 596.737 |
| K00958 | sat, met3; sulphate adenylyltransferase | 439.9 | 387.531 | 92.0289 | 32.8754 |
| K00860 | cysC; adenylylsulphate kinase | 235.256 | 226.038 | 70.0211 | 32.4492 |
| K00390 | cysH; phosphoadenosine phosphosulphate reductase | 552.209 | 485.099 | 542.678 | 523.207 |
| K05907 | APR; adenylyl-sulphate reductase (glutathione) | 58.4213 | 61.4056 | 117.009 | 39.9083 |
| K00381 | cysI; sulphite reductase (NADPH) hemoprotein beta-component | 425.422 | 469.112 | 392.07 | 499.862 |
| K00392 | sir; sulphite reductase (ferredoxin) | 4.03926 | 5.66265 | 92.1949 | 14.5694 |
| K00380 | cysJ; sulphite reductase (NADPH) flavoprotein alpha-component | 354.561 | 292.267 | 326.662 | 478.751 |
| K00640 | cysE; serine O-acetyltransferase | 841.051 | 728.585 | 598.338 | 609.716 |
| K19726 | dcsE; serine/homoserine O-acetyltransferase | 0.05834 | 0.48192 | 33.645 | 34.4534 |
| K01738 | cysK; cysteine synthase A | 469.352 | 427.524 | 669.672 | 637.288 |
| K10150 | cysO; cysteine synthase | 6.12597 | 5.12271 | 45.6951 | 17.4564 |
| K13034 | ATCYSC1; L-3-cyanoalanine synthase | 45.2923 | 162.483 | 186.48 | 211.589 |
| K17069 | MET17; O-acetylserine sulfhydrylase | 46.0507 | 38.1457 | 75.3155 | 100.341 |

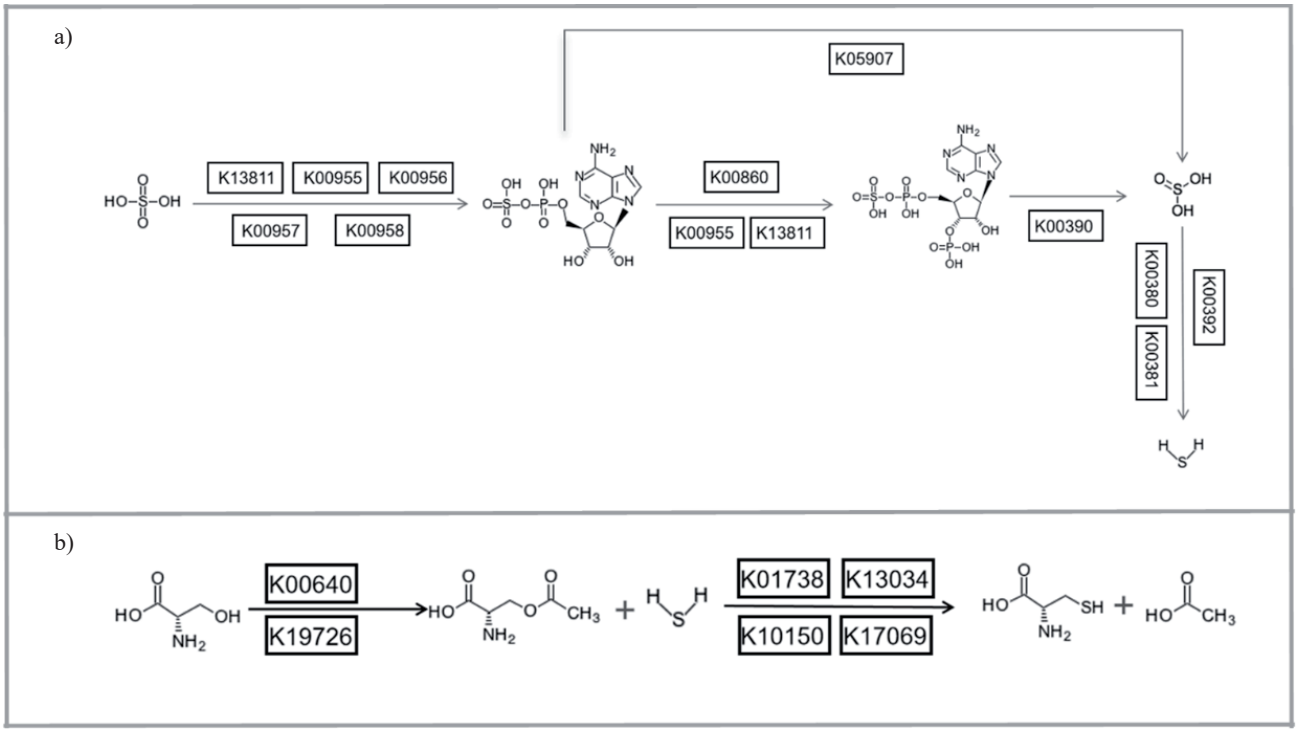


Fig. 8. a) Diagram of assimilatory sulphate reduction pathway and b) L-cysteine synthesis.

reduced ferredoxin to generate ferredoxin oxidation and hydrogen sulphide under the action of enzyme K00392. Gigolashvili et al. [39] investigated the intracellular and intercellular transport of a series of sulphur-containing metabolites as well as their long-distance transport. They found that sulphur is usually taken up by roots as sulphate to enter the sulphur metabolic pathway, which is catalysed by ATP-sulphurylase to produce 5-phosphosulfoadenosine. Subsequently, sulphite ions are catalysed by APS sulfotransferase, and sulphur compounds such as $H_2S$ are generated by sulphite reductase.

The last step of sulphate assimilation is L-cysteine synthesis. L-cysteine is a nutritional semi-essential amino acid that exists mainly as L-cystine in the extracellular space. Microorganisms meet their amino acid requirements by reacting $H_2S$ with O-acetylserine to produce L-cysteine, catalysed by the enzyme cysteine synthase (CysK or CysM), which is referred to as the SAT pathway [40]. This pathway is widely found in microorganisms such as bacteria and fungi [41]. Based on this, the enzymes involved in the conversion of serine to cysteine were searched in the KEGG database and found to be an exact match, so it is possible that sulphate assimilation may also involve cysteine synthesis. As shown in Fig. 8b), first, L-serine reacts with acetyl coenzyme A in the presence of enzymes K00640 and K19726 to form O-acetyl-L-serine and coenzyme A. Subsequently, O-acetyl-L-serine reacts with hydrogen sulphide in the enzymes K01738, K10150, K13034, and K17069 to produce L-cysteine and acetate. Nakatani et al. [42] found two L-cysteine biosynthesis pathways in *Escherichia coli*. One is the synthesis of L-cysteine from O-acetyl-L-serine (OAS) and sulphate via L-cysteine synthase (CysK). This is consistent with the predicted L-cysteine synthesis pathway.

## Conclusions

In this paper, 16s rRNA high-throughput sequencing was used to analyse microbial changes in the sludge and to explore microbial succession and sulphur metabolic pathways. Thiobios and *Thiobacillus* survived at higher sulphur concentrations and may undergo corresponding community succession. Sulphate content is inextricably linked to *Thiobacillus* and Thiobios. The SO metabolic pathway is involved in the microbial conversion of sulphite. M00176 contains all the related enzyme genes and completes the sulphur reduction pathway. This study contributes to understanding the microbial sulphur cycle in the biological treatment of oily wastewater from ships. The identified sulphur-related bacterial genera and metabolic pathways can serve as potential biological indicators for process monitoring. The research results can provide a basis for optimising the biological treatment of oily wastewater from ships, including wastewater from scrubbers. Nevertheless, further study is needed to determine the main water quality indicators influencing the microbial metabolic pathways of sulphur, as well as the importance ranking of these indicators. Furthermore, longer-term tracking of the wastewater treatment parameters in this plant and additional treatment plants for oily wastewater

from ships is needed to enhance the robustness and generalisability of the findings in this study.

## Acknowledgements

Shanghai Pujiang Programme (23PJD039), Pudong New Area Livelihood Project (PKJ2023-C01).

## AI usage Disclosure Statement

During the preparation of this manuscript, the authors used ChatGPT (OpenAI, GPT-5.5) solely for language editing to improve the academic English, readability, and clarity of the text. All AI-generated suggestions were carefully reviewed, verified, and revised by the authors. The authors take full responsibility for the content of the published manuscript.

## Conflict of Interest

The authors declare no conflict of interest.

## References

1. GRYTA M. Bilge water separation by membrane distillation. Separation and Purification Technology, **237**, 116332, **2020**.
2. ZIS T.P., CULLINANE K. The desulphurisation of shipping: Past, present and the future under a global cap. Transportation Research Part D: Transport and Environment, **82**, 102316, **2020**.
3. BACH M., SCHOENBRUNN F. Liquid-Solid Separation: De-Sanding-Flocculation, Sedimentation and Liquor Filtration. In: RAAHAUGE B.E., WILLIAMS F.S. (eds) Smelter Grade Alumina from Bauxite: History, Best Practices, and Future Challenges, Springer Series in Materials Science, Springer, Cham.: **320**, 241, **2022**.
4. VARJANI S., JOSHI R., SRIVASTAVA V.K., NGO H.H., GUO W. Treatment of wastewater from petroleum industry: current practices and perspectives. Environmental Science and Pollution Research, **27** (22), 27172, **2020**.
5. ELKAIME H., ELHAQ S.L., LOUKILI A. A Review and Current Practices on the Valorization of Ship-Generated Oily Waste. IFAC-PapersOnLine. **58** (13), 817, **2024**.
6. CHIPASA K.B. Limits of physicochemical treatment of wastewater in the vegetable oil refining industry. Polish Journal of Environmental Studies, **10** (3), 141, **2001**.
7. KANG Z. Biological treatment of wastewater from heavy oil recovery. Petroleum Science and Technology, **32** (9), 1065, **2014**.
8. VYRIDES I., DRAKOU E.-M., IOANNOU S., MICHAEL F., GATIDOU G., STASINAKIS A.S. Biodegradation of bilge water: Batch test under anaerobic and aerobic conditions and performance of three pilot aerobic Moving Bed Biofilm Reactors (MBBRs) at different filling fractions. Journal of Environmental Management, **217**, 356, **2018**.
9. ZHANG A., GAO C., CHEN T., XIE Y., WANG X. Treatment of fracturing wastewater by anaerobic granular sludge: The short-term effect of salinity and its mechanism. Bioresource Technology, **345**, 126538, **2022**.
10. HU X., LIU J., LIU H., ZHUANG G., XUN L. Sulphur metabolism by marine heterotrophic bacteria involved in sulphur cycling in the ocean. Science China Earth Sciences, **61** (10), 1369, **2018**.
11. HÖYTIÄ H.M.A., KARHU J.A., PELTONEN P.T., O'BRIEN H., HALKOAHO T., MYLLYPERKIÖ M. Isotope records of carbon, oxygen and sulphur reveal the role of sulphate evaporites in the formation of Sakatti Cu-Ni-PGE sulphide ore, Central Lapland Greenstone belt, Finland. Ore Geology Reviews, **190**, 107159, **2026**.
12. ZHANG T.-T., OO E.M.M., CHEN B.-L., LIU L., ZHAO Q.-B., YANG J.-C.E., ZHENG Y.-M. Machine learning coupling microbial succession to decipher gas stripping-reinforced sulphate reduction for hydrogen sulphide removal. Bioresource Technology, **438**, 133169, **2025**.
13. TIAN W., ZHAO Y., SUN H., BAI J., WANG Y., WU C. The effect of irrigation with oil-polluted water on microbial communities in estuarine reed rhizosphere soils. Ecological Engineering, **70**, 275, **2014**.
14. WANG J., ZHANG Y., DING Y., SONG H., LIU T., ZHANG Y., XU W., SHI Y. Comparing the indigenous microorganism system in typical petroleum-contaminated groundwater. Chemosphere, **311**, 137173, **2023**.
15. KASHIF M., LIANG Q., MENG C., LI T., LUO Y., GUO F., WANG D., JIANG C. Ecological and functional diversity of sulphur-oxidising and sulphate-reducing bacteria in Chinese mangrove ecosystems: A comparative review with insights from Guangxi Beihai. Rhizosphere, **37**, 101260, **2026**.
16. SU Z., ZHAO J., LU Z., WANG M., GUO C., SONG X., GUO X., CAI M., WU Z. The effects of different temperature conditions on sludge characteristics and microbial communities of nitritation denitrification. Journal of Water Process Engineering, **50**, 103283, **2022**.
17. SPOSOB M., CYDZIK-KWIATKOWSKA A., BAKKE R., DINAMARCA C. Temperature-induced changes in a microbial community under autotrophic denitrification with sulphide. Process Biochemistry, **69**, 161, **2018**.
18. CHEN Y., WANG S., GU J., ZHAN M., YU R. Potential applications, mechanisms and influencing factors of sulphate-reducing bacteria in soil and groundwater bioremediation: A review. Applied Soil Ecology, **221**, 106912, **2026**.
19. MALTSEVA A.I., ELCHENINOV A.G., KLYUKINA A.A., KUCHIERSKAYA A.A., LEBEDINSKY A.V., FROLOV E.N. Heterotrophic lifestyle in the phylum Thermodesulfobiota revealed by physiological and genomic characterization of the acidophilic sulphate-reducing bacterium Thermodesulfobium fumaratoxidans sp. nov. Systematic and Applied Microbiology, **49** (1), 126684, **2026**.
20. FRENCH K.L., HACKLEY P.C., SPERLING E.A. Differentiating persistent and intermittent euxinia from the molecular derivatives of green sulphur bacteria carotenoids. Geochimica et Cosmochimica Acta, **415**, 130, **2026**.
21. HEGE D., GEMMECKER Y., CLERMONT L., ALEKSIC I., OLEKSY G., SZALENIEC M., HEIDER J. Chapter Eight - Genetic manipulation of the betaproteobacterial genera Thauera and Aromatoleum. In Methods in

Enzymology, D. Tischler Ed. Academic Press, **714**, 139, **2025**.
22. KIM M., CHA I.-T., LEE K.-E., LI M., PARK S.-J. Pangenome analysis provides insights into the genetic diversity, metabolic versatility, and evolution of the genus Flavobacterium. Microbiology Spectrum, **11** (5), e01003, **2023**.
23. TIEMBLO-MARTÍN M., PISTORIO V., SAAKE P., MAHDI L., CAMPANERO-RHODES M.A., DI GIROLAMO R., DI CARLUCCIO C., MARCHETTI R., MOLINARO A., SOLÍS D., ZUCCARO A., SILIPO A. Structure and properties of the exopolysaccharide isolated from Flavobacterium sp. Root935. Carbohydrate Polymers, **343**, 122433, **2024**.
24. HUANG C., LIU Q., CHEN X., NAN J., LI Z., WANG A. Bioaugmentation with Thiobacillus sp. H1 in an autotrophic denitrification desulphurization microbial reactor: microbial community changes and relationship. Environmental Research, **189**, 109927, **2020**.
25. YANG Z., GUO F., WANG Q., ZHAO J., WANG Y., ZHU X., MAO Y., WU J., SONG Z., HU H., PENG W., LIU B. Diversity of activated sludge microbial community structure in different wastewater treatment plants. Biology Bulletin, **50** (3), 329, **2023**.
26. YE J., ZHU Y., CHEN H., ZHAO X., TANG J., ZHANG J., CHEN Y., GUO Y., TAN Y., ZHANG T. High-throughput absolute quantification sequencing reveals the adaptive succession and assembly pattern of plastisphere communities in municipal sewer systems: Influence of environmental factors and microplastic polymer types. Environmental Pollution, **342**, 123136, **2024**.
27. MARIE V., LIN J. Microbial indicators and environmental relationships in the Umhlangane River, Durban, South Africa. Open Life Sciences, **13** (1), 385, **2018**.
28. QI Y., ZHONG Y., LUO L., HE J., FENG B., ZHANG X., XIA Y., REN H. Feasibility analysis of reclaimed water reuse based on water quality data and microbial community structure study. Science of The Total Environment, **951**, 174781, **2024**.
29. JIN Z., LIANG L., ZHAO Z., ZHANG Y. Enhancing assimilatory sulphate reduction with ferrihydrite-humic acid coprecipitate in anaerobic sulphate-containing wastewater treatment. Bioresource Technology, **411**, 131308, **2024**.
30. WOO W.H., YANG H., WONG K.P., HALLIWELL B. Sulphite oxidase gene expression in human brain and in other human and rat tissues. Biochemical and Biophysical Research Communications, **305** (3), 619, **2003**.
31. CORPAS F.J., TABOADA J., SÁNCHEZ-ROMERA B., LÓPEZ-JARAMILLO J., PALMA J.M. Peroxisomal Sulphite Oxidase (SOX), an alternative source of NO in higher plants which is upregulated by H2S. Plant Physiology and Biochemistry, **225**, 110000, **2025**.
32. KAPPLER U. Bacterial sulphite-oxidising enzymes. Biochimica et Biophysica Acta (BBA)-Bioenergetics, **1807** (1), 1, **2011**.
33. HÄNSCH R., LANG C., RENNENBERG H., MENDEL R. Significance of plant sulphite oxidase. Plant Biology, **9** (5), 589, **2007**.
34. FENG C., TOLLIN G., ENEMARK J.H. Sulphite oxidising enzymes. Biochimica Et Biophysica Acta (BBA)-Proteins and Proteomics, **1774** (5), 527, **2007**.
35. ZHOU L., DONG N., FU M., YUE X., JIAN Y., LI H., RUSSENBERGER M., ZHUANG W.-Q. Dissimilatory sulphate reduction in an anaerobic biofilm reactor for tofu processing wastewater treatment: Bacterial community and their functional genes. Science of The Total Environment, **892**, 164579, **2023**.
36. JUVEN B.J., PIERSON M.D. Antibacterial effects of hydrogen peroxide and methods for its detection and quantitation. Journal of Food Protection, **59** (11), 1233, **1996**.
37. CHANCE B. The composition of catalase-peroxide complexes. Journal of Biological Chemistry, **179** (3), 1311, **1949**.
38. SHAN Z., ZHOU M., WANG P., YU Y., ZHANG J., WANG L., DONG A., WANG Q. An enzyme-hydrogen peroxide one-step preparation of cotton knitted fabric under low-temperature and near-neutral condition. International Journal of Biological Macromolecules, **306**, 141376, **2025**.
39. GIGOLASHVILI T., KOPRIVA S. Transporters in plant sulphur metabolism. Frontiers in Plant Science, **5**, 442, **2014**.
40. MARCHETTI M., DE ANGELIS F.S., ANNUNZIATO G., COSTANTINO G., PIERONI M., RONDA L., MOZZARELLI A., CAMPANINI B., CANNISTRARO S., BIZZARRI A.R., BETTATI S. A competitive O-acetylserine sulfhydrylase inhibitor modulates the formation of cysteine synthase complex. Catalysts, **11** (6), 700, **2021**.
41. ZHANG F., ZHU J., ZHAO Y., SHAN B., LU J., WANG H. L-cysteine-modified Ag-based nanomaterials for asymmetric electrocarboxylation of aromatic ketones. Applied Surface Science, **730**, 166357, **2026**.
42. NAKATANI T., OHTSU I., NONAKA G., WIRIYATHANAWUDHIWONG N., MORIGASAKI S., TAKAGI H. Enhancement of thioredoxin/glutaredoxin-mediated L-cysteine synthesis from S-sulfocysteine increases L-cysteine production in Escherichia coli. Microbial Cell Factories, **11**, 62, **2012**.